Conserved domains of meiosis-specific CHK2 protein in budding yeast contribute to its kinase activity

Jinsha Padmarajan, Abhijna Krishnan Edilyam, Vijayalakshmi V. Subramanian[#]

Indian Institute of Science Education and Research (IISER) Tirupati
[#]Corresponding author: viji@labs.iisertirupati.ac.in

Abstract

Programmed double strand DNA breaks in meiosis can be repaired as inter-homologue crossovers and thereby aid the faithful segregation of homologous chromosomes. Biased repair mechanisms enforce repair with the homologue. Further, DNA breaks left unrepaired lead to checkpoint activation. Meiosis-specific Chk2 kinase in budding yeast mediates the biased repair of meiotic DSBs using homologue partner but also enforces the meiotic checkpoint. Here we investigate Mek1 kinase activity in budding yeast by analyzing novel point mutants derived from an EMS mutagenesis screen. The point mutants in different domains of Mek1 abolish its activity that cannot be rescued by complementation in transheterozygotes. Our findings lend insight on the mechanism of Mek1 function during meiosis.

Introduction

Meiosis is a highly organized chromosome segregation process in sexually-reproducing organisms that generates haploid gametes from diploid progenitors (Kleckner 1996; Hochwagen 2008). Reduction in ploidy is achieved by a single round of chromosome duplication event followed by segregation of homologous chromosomes in meiosis I and that of sister chromatids in meiosis II (Kleckner 1996; Hunter 2015). Accurate homologue segregation in meiosis I entails induction of programmed double-stranded DNA breaks (DSBs) and subsequent repair as crossovers between the homologues (Subramanian and Hochwagen 2014; Lam and Keeney 2014; Hunter 2015). At least one crossover per homologue pair is required to create a physical link between them (Hochwagen 2008). This promotes proper orientation and segregation of the homologues on the meiotic spindle and preserves fertility during this process (Kleckner 1996; Hochwagen 2008).

While meiotic DSBs can potentially use either the homologue or the proximal sister chromatid as a template for repair, only repair from the homologue can give rise to crossovers that are crucial for accurate chromosome segregation (Subramanian and Hochwagen 2014; Hunter 2015). Therefore, unlike repair of DSBs in vegetative cells which primarily utilize the sister chromatid as a template (Kadyk and Hartwell 1992; Bzymek *et al.* 2010), DSBs in

meiosis preferentially repair using the homologue as a template (Hollingsworth 2010; Humphryes and Hochwagen 2014). This biased repair with the homologue template is mechanistically linked to DSB repair in meiosis (Subramanian and Hochwagen 2014). In *S. cerevisiae*, DSB ends and the 5′ end-resected single stranded DNA ends trigger conserved checkpoint kinases Tel1/Mec1 (ATM/ATR orthologues), which set the stage for downstream repair of DSBs and also promote homologue bias (Grushcow *et al.* 1999; Cheng *et al.* 2013; Penedos *et al.* 2015). Additionally repair of meiotic DSBs occurs in the context of specialized meiotic chromosomal proteins which includes meiotic cohesins, Red1, Hop1 (conserved HORMAD protein) and Mek1 kinase (Chk2 orthologue) (Hollingsworth and Byers 1989; Rockmill and Roeder 1991; Leem and Ogawa 1992; Smith and Roeder 1997; Bailis and Roeder 1998; Klein *et al.* 1999; Panizza *et al.* 2011). The checkpoint kinases (Tel1/Mec1) phosphorylate Hop1 at threonine 318 in response to DSBs (Carballo *et al.* 2008; Cheng *et al.* 2013). Phosphorylated Hop1 serves as an adaptor for Mek1 kinase localization to meiotic chromosomes (presumably at/near DSB sites), its dimerization and activation of the kinase function (Niu *et al.* 2005, 2007; Carballo *et al.* 2008; Ontoso *et al.* 2013; Subramanian *et al.* 2016).

Chk2 kinase contributes to repair choices and outcome as well as recombination checkpoint in several organisms (Subramanian and Hochwagen 2014). In budding yeast, Mek1 kinase activity is responsible for promoting homologue bias; in *mek1⊿* or upon Mek1 kinase activity inhibition, the DSBs are repaired with the sister chromatid template and result in meiosis I segregation errors (Wan *et al.* 2004; Niu *et al.* 2007). While Mek1 restricts Rad51 strand invasion activity by phosphorylating its cofactor Rad54 and interactor Hed1, other Mek1-dependent mechanisms are also at play to promote homologue bias (Liu *et al.* 2014; Callender *et al.* 2016). Additionally, Mek1 contributes to crossover interference (a mechanism to ensure non-random and well-spaced crossover placement) by targeting synaptonemal complex proteins (Chen *et al.* 2015). Similarly, a reduction in homologue crossovers is also observed in *C. elegans* Chk2 orthologues, *cds1/2* mutants (Oishi *et al.* 2001). Further, Mek1/ Chk2 facilitates meiotic recombination checkpoint and delays cell cycle progression when DSBs are unrepaired (Pérez-Hidalgo *et al.* 2008; Wu *et al.* 2010). In mouse, Chk2 is responsible for eliciting DNA damage response (Bolcun-Filas *et al.* 2014; Pacheco *et al.* 2015; Martínez-Marchal *et al.* 2020). One mechanism by which Mek1 elicits the recombination checkpoint in budding yeast is by phosphorylating and restricting the activity of Ndt80, a transcription factor that is essential for exit from meiotic prophase (Prugar *et al.* 2017; Chen *et al.* 2018).

Mek1 protein has three conserved domains with respect to Chk2; an N-terminal forkhead-association domain (FHA), a kinase domain and a C-terminal domain. Upon DSB formation, the FHA, a conserved phospho-protein binding domain of Mek1 binds to phosphorylated Hop1 (pHop1) (Durocher and Jackson 2002; Wan *et al.* 2004). Recruitment

of Mek1 by pHop1 promotes its dimerization and autophosphorylation of threonine residues in its kinase activation loop, leading to kinase activation (Wan *et al.* 2004; Niu *et al.* 2007). Specific mutations in these domains have been reported to abolish the kinase activity of Mek1 (Wan *et al.* 2004; Niu *et al.* 2007).

Here we report analysis of novel *mek1* point mutations isolated from an EMS mutagenesis screen that either carry missense mutations in the FHA or kinase domains or truncate the C-terminus. We assess Mek1 function and protein stability in these mutants. We find that in the missense mutants the protein is stably expressed and the predicted structure of the mutant protein is unchanged. On the other hand, C-terminus truncated Mek1 mutants have an altered predicted structure and accordingly exhibit reduced protein levels in meiosis. Regardless, function is severely compromised in all mutants. Finally, genetic trans-complementation of these mutants suggest that all domains are essential even *in trans* in a dimer. Our findings indicate that the conserved domains of Mek1 are key to its kinase activity and for upholding homologue bias and recombination checkpoint in meiosis.

Results and Discussion

Mek1 triggers a recombination checkpoint arrest when a meiosis specific strand invasion protein, Dmc1, is absent (Roeder and Bailis 2000; Wu *et al.* 2010). However if *MEK1* is deleted, the block on Rad51 strand invasion protein is lifted, DSBs are repaired (albeit with sister chromatids in the absence of homologue bias) and budding yeast cells complete meiosis to form gametes (spores) (Wan *et al.* 2004). Taking advantage of this mechanism, an EMS mutagenesis screen was performed to isolate mutants that bypass *dmc1* meiotic arrest (the screen will be described elsewhere). Point mutations in *mek1** were isolated from the screen and identified using genetic non-complementation with *mek1Δ* followed by sanger sequencing. Here we discuss five mutations in the three conserved domains of Mek1 (Figure 1a); one in FHA domain (S66F), two in the kinase domain (P245L, P384S) and two at the C-terminus (W410*, W443*).

Mek1 kinase sequence and domains are conserved

Mek1 is a meiosis specific checkpoint kinase with three structural domains, namely FHA domain, kinase domain and C-terminal domain (Figure 1a) (Niu *et al.* 2007). Both the FHA and kinase domains are conserved across the Chk2 kinase family. A multiple sequence alignment using ClustalW revealed that mutant sites S66 and P384 are conserved across species while P245 is beside a conserved site G246 (Figure 1b, 1c). Alphafold2 prediction of Mek1 structure showed that the kinase domain consists of alpha helices and beta strands, while 73 amino acids long FHA domain is made up of 6 beta strands (Figure 1d) (Jumper *et al.* 2021; Mirdita *et al.* 2021). Interpro protein domain prediction was done to visualize possible loss of kinase and FHA domains. Interestingly, neither the mutation in the FHA domain (S66F) nor the two missense kinase mutations P245L and P384S dramatically affect the predicted structure of Mek1 (data not shown) suggesting that protein folding may not be the cause of the mutant phenotype. The C-terminal truncation mutants W410* and W443*

have a deletion of 87 and 54 amino acids respectively. Alphafold2 predicted loss of three C-terminal alpha helices and a disordered region in W410*, while loss of one C-terminal helix and disordered region in W443* (Figure 1e). These findings suggest that the C-terminal domain of Mek1 may contribute to proper folding of Mek1 kinase.

mek1* point mutants phenocopy _mek1Δ_ mutant

The *mek1** point mutants were isolated on the basis of their ability to bypass meiotic arrest observed in *dmc1Δ*, however, the strains may have several other mutations in the background. To clearly assign the phenotype to *mek1*, we introduced each point mutation into a non-mutagenized, clean yeast background using CRISPR Cas9. The *mek1** point mutants were then assessed for their ability to bypass the recombination checkpoint in *dmc1Δ*. The point mutants rescued the sporulation defect seen in *dmc1Δ* (Figure 2a, Table S2a), suggesting that these point mutations in *mek1* abolished its recombination checkpoint activity. Additionally, none of the spores were viable (data not shown), suggesting a loss of homologue bias in the DSB repair process.

We also assessed the phenotype of *mek1** point mutants in the presence of Dmc1 strand exchange activity. No defects were observed in sporulation (Figure 2b, Tables S2b, S2c), however the spores were not viable (Table S2d). These findings indicate that *mek1** point mutants phenocopy *mek1Δ* with respect to sporulation and spore viability and exhibit a complete loss of function.

Mek1 point mutations do not dramatically affect protein stability

Because *mek1** point mutants exhibited a complete loss of function and phenocopied *mek1Δ*, we wondered if protein folding and stability were compromised leading to loss of function. To interrogate the protein levels in the *mek1** point mutants, we did a western analysis to assess levels of Mek1 protein during meiosis (Figure 3, Figure S1). We used meiosis-specific Red1 as well as Pgk1 as our loading controls. The Mek1 protein levels were similar in the missense mutants compared to wild type. These findings, in addition to absence of any predicted folding defects in these mutants, suggest that in the FHA and kinase domain mutants loss of function may be due to loss of critical interactors rather than the protein itself. The C-terminal truncation mutants, however, exhibited lower Mek1 protein levels (Figure 3, Figure S1). The predicted folding of the C-terminal truncation is also compromised. Together these observations suggest that the truncation mutants might be less stable.

Kinase activity of Mek1 point mutants is severely compromised

In FHA and kinase mutants, the protein levels were not compromised, however, these mutants phenocopied *mek1Δ*. To identify the cause of phenotypic defects in these mutants we sought to assess their kinase activity. Substrates of Mek1 include phosphorylation of histone H3 on threonine 11 (Govin *et al.* 2010; Subramanian *et al.* 2016; Kniewel *et al.* 2017). Phosphorylation of H3T11 was not observed in the FHA and kinase mutants (Figure 4, Figure S2). This lack of Mek1 activation was not because DSB formation was compromised; γ-H2AX signal (a marker downstream of DSBs) was similar to controls (Figure 4, Figure S2). Very low levels of pH3T11 signal was observed in C-terminal truncation (W443*, see Figure S2) also pointing to why these cells exhibited mutant phenotype. These findings are

consistent with previous reports (Wan *et al.* 2004; Niu *et al.* 2007), where point mutations in the FHA domain or the C-terminal regions caused loss of Mek1 activity.

Transheterozygotes of *mek1* point mutants do not rescue the mutant phenotype

None of the *mek1** mutants analyzed so far were functionally competent. However, because the Mek1 function *in vivo* requires its dimerization, one possibility is that the mutations in different domains may complement each other *in trans* following dimerization. To examine complementation between different alleles *in trans*, we generated *dmc1Δ* transheterozygotes. We did observed a rescue of *dmc1Δ* meiotic arrest suggesting that each of these domains are critical for Mek1 function even within a dimer. It is also possible that these domains are important for dimerization itself. Indeed ectopic dimerization rescued function of point mutations in FHA and C-terminus of Mek1 (Wan *et al.* 2004; Niu *et al.* 2007).

Our work has investigated novel *mek1* mutants. We have found that each of the Mek1 domains are critical for its function. The mutants are unable to impose recombination checkpoint or homologue bias. Interestingly the mutants are also able to rescue the *dmc1* arrest *in trans* indicative of lack of Mek1 activity. Further analysis of these mutants will shed light on the mechanisms of Mek1-mediated homologue bias and checkpoint.

Materials and methods

Strains

All experiments were performed using strains in the SK1 background. The list of strains can be found in Table S1.

*mek1** point mutant strains were derived from a random EMS (Ethyl methanesulfonate) mutagenesis of *dmc1* mutants. The *mek1** gene amplicon of the mutant alleles were transformed into a non-mutagenized genetic background (*mek1Δ::kanMX*) along with CRISPR Cas9 plasmid also carrying guide RNA targeting *KanMX* (pRS425-*Cas9-sg-KanMX*). The cells were plated on leucine-dropout (DO) selection media to select for cells transformed with the Cas9 plasmid which would cleave at the *KanMX* sequence. The obtained transformants were streaked on YPD media to lose the plasmid. *mek1** point mutants clones for further study clones were chosen on the basis of negative selection on both leucine-DO and G418 drug plates. The *mek1** point mutants were mated with a *mek1* null strain in *dmc1* as well as *DMC1* background and the obtained diploids were used for functional assays.

Structure and functional domain prediction and alignment of Mek1

Structure prediction of proteins was done using Deepmind's Alphafold2, using the open access alphafold2_advanced script (https://colab.research.google.com/github/sokrypton/ColabFold/blob/main/beta/AlphaFold2_advanced.ipynb)(Jumper *et al.* 2021; Mirdita *et al.* 2021). Mmseq2 was used as multiple alignment tool for all the predictions with rest of the parameters as default. This method was used to generate five predicted models with output as pdb file. The ranks were assigned based on the pLDDT score, and the model with the highest rank was used for further analysis. The

generated alpha fold structures were visualised using pymol (Schrodinger, LLC. 2010. The PyMOL Molecular Graphics System, Version 1.20). Protein domain prediction of mutants was done using EBI's InterPro (https://www.ebi.ac.uk/interpro/). Multiple sequence alignment was done online using the MAFFT tool from EBI website (https://www.ebi.ac.uk/Tools/msa/mafft/) and visualised using Jalview(Waterhouse *et al.* 2009). Sequences were sorted based on pairwise identity with Mek1 from *S cerevisiae* (SK1) as reference sequence.

Synchronous meiosis

Freshly patched diploid strains on YPG were inoculated in YPD culture and grown at room temperature while shaking at 200rpm for 24hrs. Cells were diluted in 50ml BYTA (50mM sodium phthalate-buffered, 1% yeast extract, 2% tryptone and 1% acetate) to a final A_{600}=0.3 and incubated for 16hrs at 30°C at 200rpm. Meiosis was induced in sporulation media (0.3% potassium acetate, 5% acetic acid) by diluting the cells to an O.D of 2. Culture was incubated at 30°C at 200rpm and samples were collected at desired time points.

Sporulation and spore viability assays

Sporulation of the diploid strains were monitored after 24hrs of meiotic induction. For each biological replicate, a total of 200 spores were counted and are shown as a percentage of sporulated cells from a population of cells to obtain sporulation efficiency. For spore viability, 20µl sporulated samples were added to equal volume of 1mg/ml Zymolyase T-100 and incubated at 37°C for 30 mins. Zymolase treated tetrads were dissected and the spores were allowed to germinate on growth media for two days. Spore viability was determined as the percentage of viables spore clones from total spores dissected. The graphs for sporulation efficiency and spore viability for the the diploid mutants strains along with controls were plotted using R version 4.2.2.

Whole-cell protein extraction and Western blot analysis

For protein extraction, 5ml of samples were collected from the sporulating culture at required time intervals. The cell pellets were resuspended in 5ml of 5% trichloro acetic acid (TCA). Cells were then washed in 1M unbuffered Tris and resuspended in TE (50mM Tris pH 7.5, 1mM EDTA) + DTT (200mM final concentration) master mix. Samples were boiled at 95°C for 5 min in SDS sample buffer and stored at -20°C for long term storage. Protein samples were resolved on SDS-PAGE followed by transfer onto nitrocellulose membrane at a constant voltage of 100V for 1hr. Mek1 and Red1 proteins were resolved on an 8% acrylamide resolving gel whereas phosphorylated histones were resolved on a 15% acrylamide gel.

Antibodies

The details of primary and secondary antibodies used in this study are listed in supplementary table S3.

Trans-complementation with *mek1 mutants**

Patches of each *mek1** point mutant in a *MATa dmc1 ade2 LEU2* background was replica-plated onto a lawn of each *mek1** point mutant in a *MATa dmc1 ade2 LEU2*. Diploids

were selected on adenine-leucine-DO media. The diploids thus formed were transferred onto Protran BA85 nitrocellulose blotting membrane on adenine-leucine-DO selective media by replica plating. The plates were incubated at 30°C until a good amount of cells were grown on the membrane. The membranes were then transferred onto MSM plates (2% KOAc/AcAcid) to induce sporulation at 30°C for 4-5 days. The plates were screened under short UV for the presence of fluorescent patches (spores have a di-tyrosine component that fluoresces under UV light).

Acknowledgements

We thank Andreas Hochwagen for generously sharing *mek1* mutants from the EMS mutagenesis screen. This work was supported in part by Ramalingaswami re-entry fellowship (BT/RLF/Re-entry/04/2019), DBT-Wellcome Trust India Alliance intermediate fellowship (IA/I/21/1/505647), SERB CRG grant (CRG/2021/007107/BHS) to V.V.S., and CSIR-JRF fellowship (09/1178(12250)/2021-EMR-I) to A.K.E.

Table 1: Trans-complementation between *mek1 point mutants**

Mek1 genotype	*mek1Δ*	*MEK1+*	*mek1*S66F*	*mek1*P245L*	*mek1*P384S*	*mek1*W410**	*mek1*W443**
mek1Δ	S	NS	S	S	S	S	S
MEK1+	NS	NS	NS	NS	NS	NS	NS
mek1*S66F	S	NS	S	S	S	S	S
mek1*P245L	S	NS	S	S	S	S	S
mek1*P384S	S	NS	S	S	S	S	S
mek1*W410*	S	NS	S	S	S	S	S
mek1*W443*	S	NS	S	S	S	S	S

References

Bailis J. M., and G. S. Roeder, 1998 Synaptonemal complex morphogenesis and sister-chromatid cohesion require Mek1-dependent phosphorylation of a meiotic chromosomal protein. Genes Dev. 12: 3551–3563.

Bolcun-Filas E., V. D. Rinaldi, M. E. White, and J. C. Schimenti, 2014 Reversal of female infertility by Chk2 ablation reveals the oocyte DNA damage checkpoint pathway. Science 343: 533–536.

Bzymek M., N. H. Thayer, S. D. Oh, N. Kleckner, and N. Hunter, 2010 Double Holliday junctions are intermediates of DNA break repair. Nature 464: 937–941.

Callender T. L., R. Laureau, L. Wan, X. Chen, R. Sandhu, *et al.*, 2016 Mek1 Down Regulates Rad51 Activity during Yeast Meiosis by Phosphorylation of Hed1. PLoS Genet. 12: e1006226.

Carballo J. A., A. L. Johnson, S. G. Sedgwick, and R. S. Cha, 2008 Phosphorylation of the axial element protein Hop1 by Mec1/Tel1 ensures meiotic interhomolog recombination. Cell 132: 758–770.

Chen X., R. T. Suhandynata, R. Sandhu, B. Rockmill, N. Mohibullah, *et al.*, 2015 Phosphorylation of the Synaptonemal Complex Protein Zip1 Regulates the Crossover/Noncrossover Decision during Yeast Meiosis. PLoS Biol. 13: e1002329.

Chen X., R. Gaglione, T. Leong, L. Bednor, T. de Los Santos, *et al.*, 2018 Mek1 coordinates meiotic progression with DNA break repair by directly phosphorylating and inhibiting the yeast pachytene exit regulator Ndt80. PLoS Genet. 14: e1007832.

Cheng Y.-H., C.-N. Chuang, H.-J. Shen, F.-M. Lin, and T.-F. Wang, 2013 Three distinct modes of Mec1/ATR and Tel1/ATM activation illustrate differential checkpoint targeting during budding yeast early meiosis. Mol. Cell. Biol. 33: 3365–3376.

Durocher D., and S. P. Jackson, 2002 The FHA domain. FEBS Lett. 513: 58–66.

Govin J., J. Dorsey, J. Gaucher, S. Rousseaux, S. Khochbin, *et al.*, 2010 Systematic screen reveals

new functional dynamics of histones H3 and H4 during gametogenesis. Genes Dev. 24: 1772–1786.

Grushcow J. M., T. M. Holzen, K. J. Park, T. Weinert, M. Lichten, *et al.*, 1999 Saccharomyces cerevisiae checkpoint genes MEC1, RAD17 and RAD24 are required for normal meiotic recombination partner choice. Genetics 153: 607–620.

Hochwagen A., 2008 Meiosis. Curr. Biol. 18: R641–R645.

Hollingsworth N. M., and B. Byers, 1989 HOP1: a yeast meiotic pairing gene. Genetics 121: 445–462.

Hollingsworth N. M., 2010 Phosphorylation and the creation of interhomolog bias during meiosis in yeast. Cell Cycle 9: 436–437.

Humphryes N., and A. Hochwagen, 2014 A non-sister act: recombination template choice during meiosis. Exp. Cell Res. 329: 53–60.

Hunter N., 2015 Meiotic Recombination: The Essence of Heredity. Cold Spring Harb. Perspect. Biol. 7. https://doi.org/10.1101/cshperspect.a016618

Jumper J., R. Evans, A. Pritzel, T. Green, M. Figurnov, *et al.*, 2021 Highly accurate protein structure prediction with AlphaFold. Nature 596: 583–589.

Kadyk L. C., and L. H. Hartwell, 1992 Sister chromatids are preferred over homologs as substrates for recombinational repair in Saccharomyces cerevisiae. Genetics 132: 387–402.

Kleckner N., 1996 Meiosis: how could it work? Proc. Natl. Acad. Sci. U. S. A. 93: 8167–8174.

Klein F., P. Mahr, M. Galova, S. B. Buonomo, C. Michaelis, *et al.*, 1999 A central role for cohesins in sister chromatid cohesion, formation of axial elements, and recombination during yeast meiosis. Cell 98: 91–103.

Kniewel R., H. Murakami, Y. Liu, M. Ito, K. Ohta, *et al.*, 2017 Histone H3 Threonine 11

Phosphorylation Is Catalyzed Directly by the Meiosis-Specific Kinase Mek1 and Provides a Molecular Readout of Mek1 Activity in Vivo. Genetics 207: 1313–1333.

Lam I., and S. Keeney, 2014 Mechanism and regulation of meiotic recombination initiation. Cold Spring Harb. Perspect. Biol. 7: a016634.

Leem S. H., and H. Ogawa, 1992 The MRE4 gene encodes a novel protein kinase homologue required for meiotic recombination in Saccharomyces cerevisiae. Nucleic Acids Res. 20: 449–457.

Liu Y., W. A. Gaines, T. Callender, V. Busygina, A. Oke, *et al.*, 2014 Down-regulation of Rad51 activity during meiosis in yeast prevents competition with Dmc1 for repair of double-strand breaks. PLoS Genet. 10: e1004005.

Martínez-Marchal A., Y. Huang, M. T. Guillot-Ferriols, M. Ferrer-Roda, A. Guixé, *et al.*, 2020 The DNA damage response is required for oocyte cyst breakdown and follicle formation in mice. PLoS Genet. 16: e1009067.

Mirdita M., S. Ovchinnikov, and M. Steinegger, 2021 ColabFold - Making protein folding accessible to all. bioRxiv 2021.08.15.456425.

Niu H., L. Wan, B. Baumgartner, D. Schaefer, J. Loidl, *et al.*, 2005 Partner choice during meiosis is regulated by Hop1-promoted dimerization of Mek1. Mol. Biol. Cell 16: 5804–5818.

Niu H., X. Li, E. Job, C. Park, D. Moazed, *et al.*, 2007 Mek1 kinase is regulated to suppress double-strand break repair between sister chromatids during budding yeast meiosis. Mol. Cell. Biol. 27: 5456–5467.

Oishi I., K. Iwai, Y. Kagohashi, H. Fujimoto, K. Kariya, *et al.*, 2001 Critical role of Caenorhabditis elegans homologs of Cds1 (Chk2)-related kinases in meiotic recombination. Mol. Cell. Biol. 21: 1329–1335.

Ontoso D., I. Acosta, F. van Leeuwen, R. Freire, and P. A. San-Segundo, 2013 Dot1-dependent histone H3K79 methylation promotes activation of the Mek1 meiotic checkpoint effector kinase

by regulating the Hop1 adaptor. PLoS Genet. 9: e1003262.

Pacheco S., M. Marcet-Ortega, J. Lange, M. Jasin, S. Keeney, *et al.*, 2015 The ATM signaling cascade promotes recombination-dependent pachytene arrest in mouse spermatocytes. PLoS Genet. 11: e1005017.

Panizza S., M. A. Mendoza, M. Berlinger, L. Huang, A. Nicolas, *et al.*, 2011 Spo11-accessory proteins link double-strand break sites to the chromosome axis in early meiotic recombination. Cell 146: 372–383.

Penedos A., A. L. Johnson, E. Strong, A. S. Goldman, J. A. Carballo, *et al.*, 2015 Essential and Checkpoint Functions of Budding Yeast ATM and ATR during Meiotic Prophase Are Facilitated by Differential Phosphorylation of a Meiotic Adaptor Protein, Hop1. PLoS One 10: e0134297.

Pérez-Hidalgo L., S. Moreno, and P. A. San-Segundo, 2008 The fission yeast meiotic checkpoint kinase Mek1 regulates nuclear localization of Cdc25 by phosphorylation. Cell Cycle 7: 3720–3730.

Prugar E., C. Burnett, X. Chen, and N. M. Hollingsworth, 2017 Coordination of Double Strand Break Repair and Meiotic Progression in Yeast by a Mek1-Ndt80 Negative Feedback Loop. Genetics 206: 497–512.

Rockmill B., and G. S. Roeder, 1991 A meiosis-specific protein kinase homolog required for chromosome synapsis and recombination. Genes Dev. 5: 2392–2404.

Roeder G. S., and J. M. Bailis, 2000 The pachytene checkpoint. Trends Genet. 16: 395–403.

Smith A. V., and G. S. Roeder, 1997 The yeast Red1 protein localizes to the cores of meiotic chromosomes. J. Cell Biol. 136: 957–967.

Subramanian V. V., and A. Hochwagen, 2014 The meiotic checkpoint network: step-by-step through meiotic prophase. Cold Spring Harb. Perspect. Biol. 6: a016675.

Subramanian V. V., A. J. MacQueen, G. Vader, M. Shinohara, A. Sanchez, *et al.*, 2016 Chromosome Synapsis Alleviates Mek1-Dependent Suppression of Meiotic DNA Repair. PLoS Biol. 14: e1002369.

Wan L., T. de los Santos, C. Zhang, K. Shokat, and N. M. Hollingsworth, 2004 Mek1 Kinase Activity Functions Downstream of RED1 in the Regulation of Meiotic Double Strand Break Repair in Budding Yeast. MBoC 15: 11–23.

Waterhouse A. M., J. B. Procter, D. M. A. Martin, M. Clamp, and G. J. Barton, 2009 Jalview Version 2—a multiple sequence alignment editor and analysis workbench. Bioinformatics 25: 1189–1191.

Wu H.-Y., H.-C. Ho, and S. M. Burgess, 2010 Mek1 kinase governs outcomes of meiotic recombination and the checkpoint response. Curr. Biol. 20: 1707–1716.

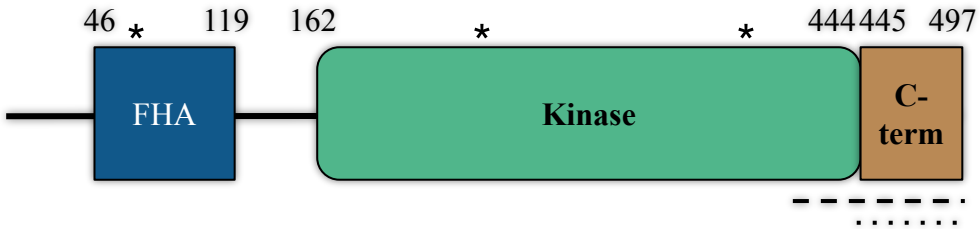

Figure 1: Sequence conservation and structure

a) Mek1 consists of FHA domain, catalytically active kinase domain and a conserved C-terminal domain; ∗ denotes position of point mutations (S66F, P245L, P384S), dashed and dotted lines denotes W410* and W443* truncations respectively.

FHA domain

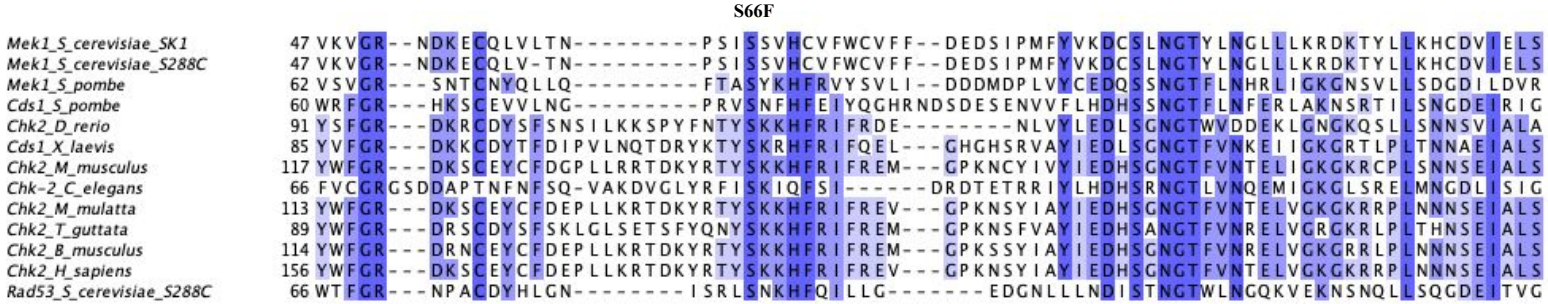

Figure 1: Sequence conservation and structure

b) Multiple sequence alignment of FHA domain; the position of the point mutation S66F is indicated

Kinase domain

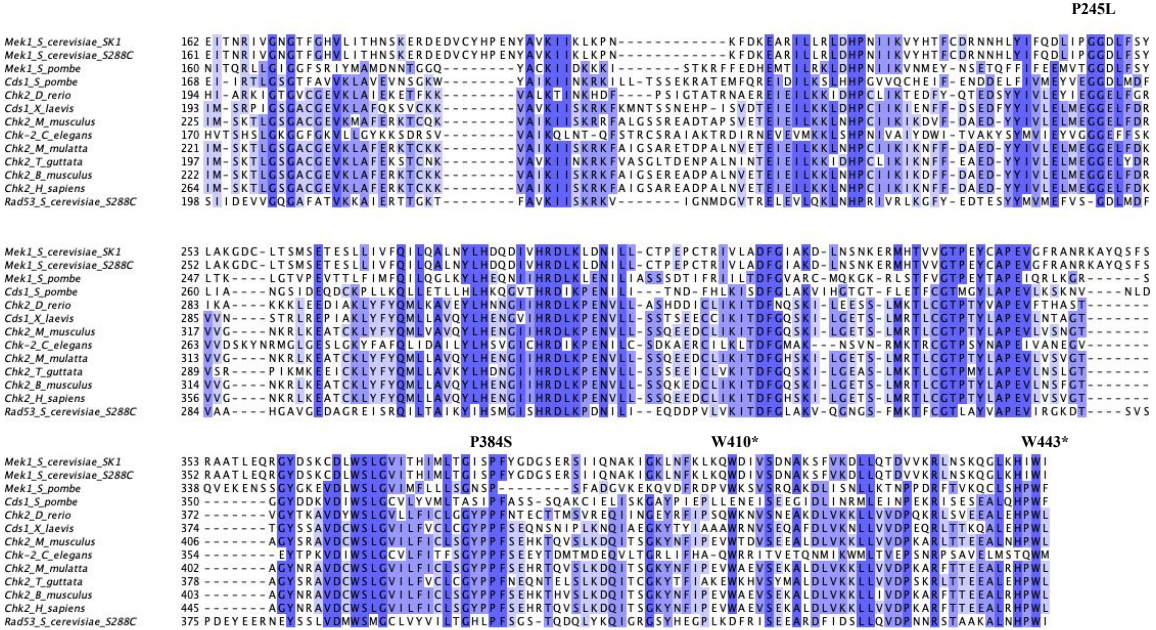

Figure 1: Sequence conservation and structure

c) Multiple sequence alignment of the kinase domain; the position of the point mutations (P245L, P384S) and truncations (W410*, W443*) are indicated.

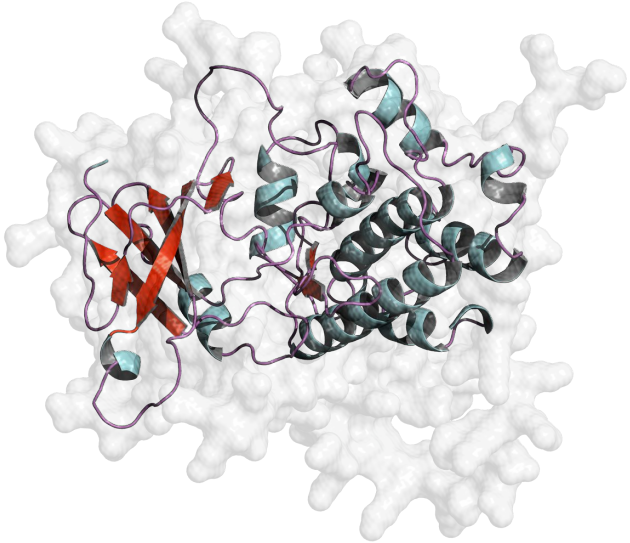

Kinase domain

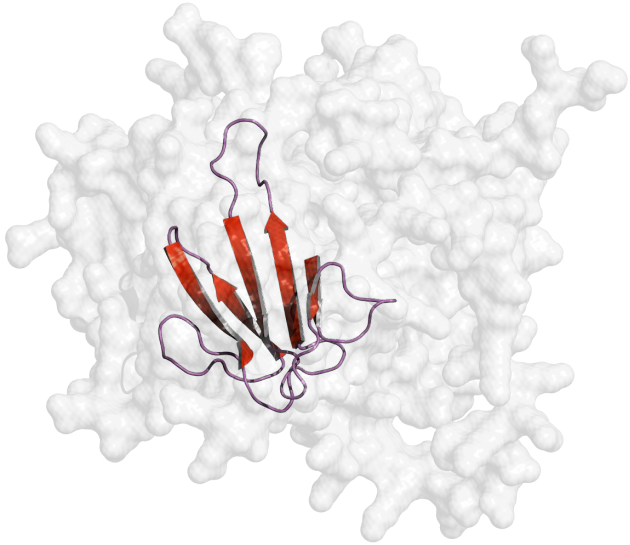

FHA domain

Figure 1: Sequence conservation and structure

e) Alphafold2 predicted structures of kinase domain and FHA domain**.** The models are coloured based on secondary structures.

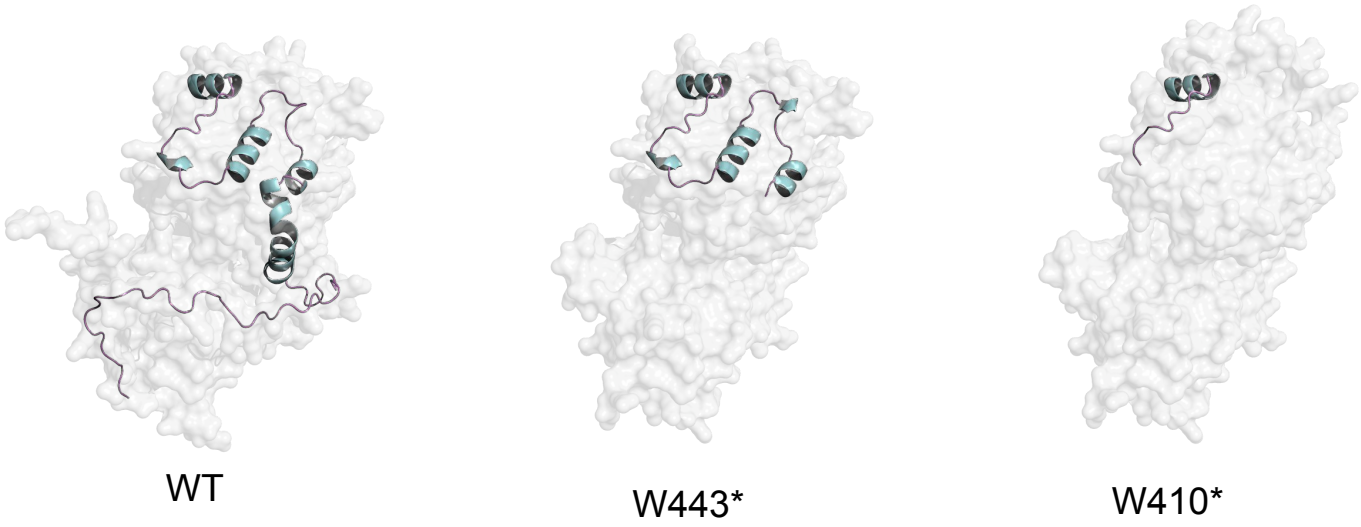

Figure 1: Sequence conservation and structure
f) Alphafold2 predicted C-terminal regions of wild type, Mek1-W443*, Mek1-W410*. C-terminal regions are highlighted as helices connected by loops using pymol. Mek1 C-terminal truncation mutants lack the C-terminal alpha helix and a disordered region compared to wild type.

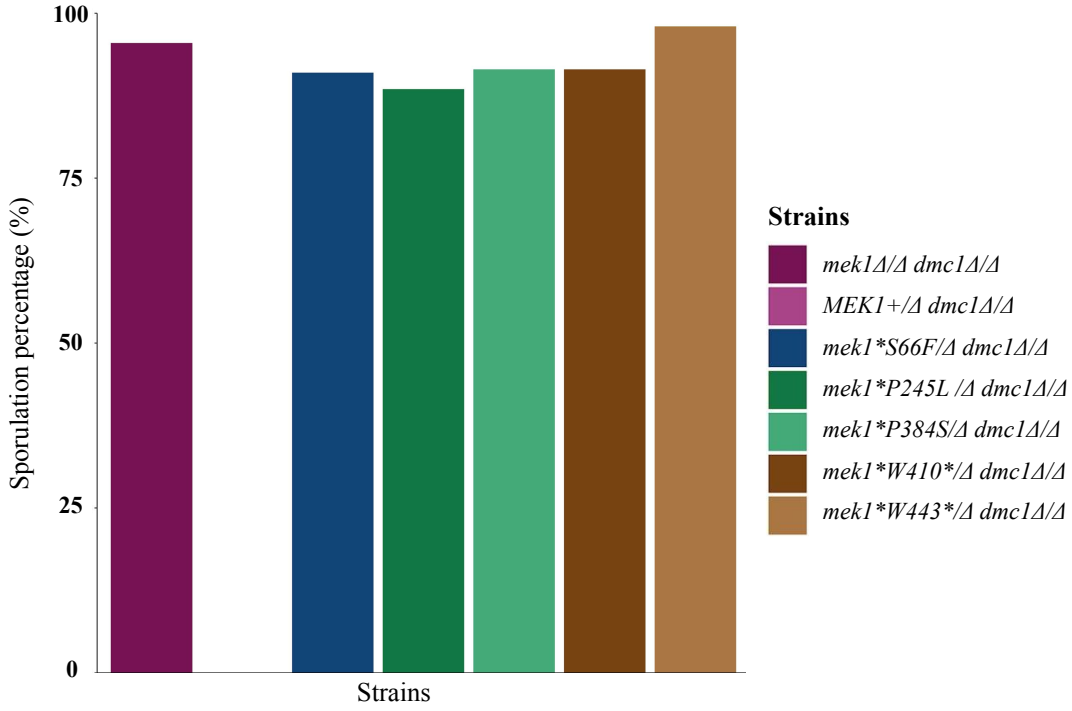

Figure 2: Sporulation efficiency and spore viability in *mek1* dmc1* and *mek1* DMC1* cells

a) Sporulation efficiency was defined as the percentage of the number of spores to the total number of cells counted. Sporulation efficiency of *mek1** point mutants along with control in *dmc1* background was calculated for n=200 for each of the indicated strains.

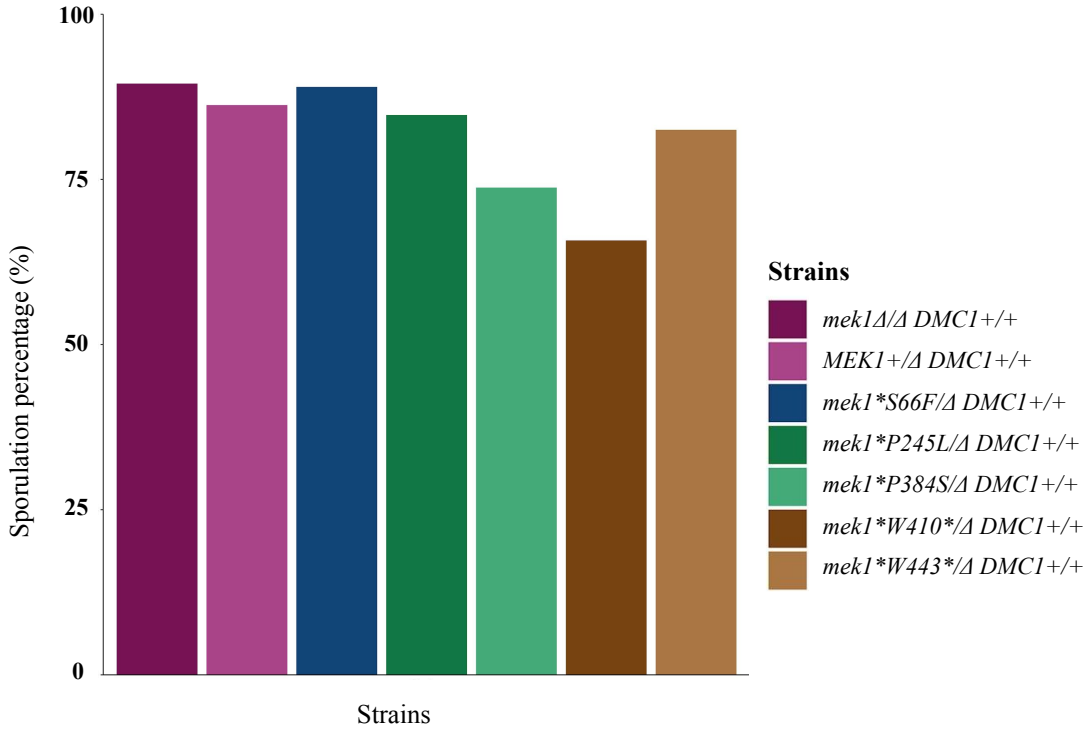

Figure 2: Sporulation efficiency and spore viability in *mek1* dmc1* and *mek1* DMC1* cells

b) Sporulation efficiency of *mek1** point mutants in DMC1 background was calculated as an average from 2 biological replicates for n=200 for each of the indicated strains.

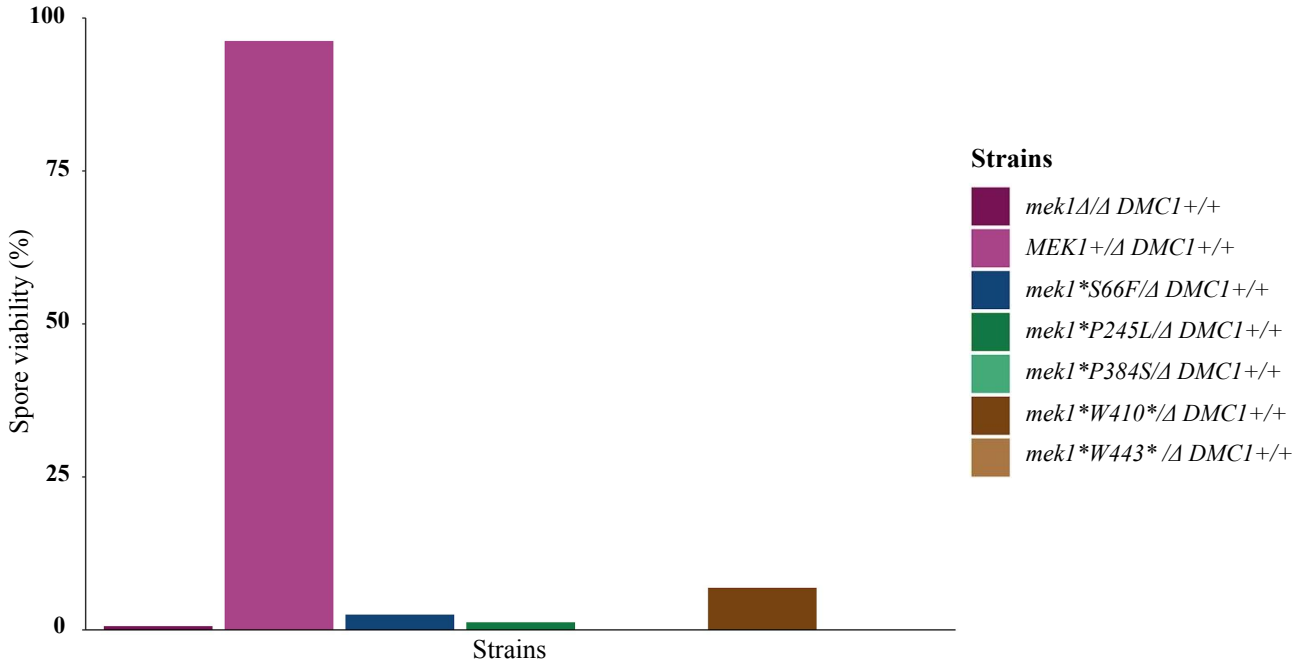

Figure 2: Sporulation efficiency and spore viability in *mek1* dmc1* and *mek1* DMC1* cells

c) Spore viability was defined as the percentage ratio of number of spores that are viable divided by the total number of spores dissected. The experiment was done for the indicated strains for one biological replicate for n=40.

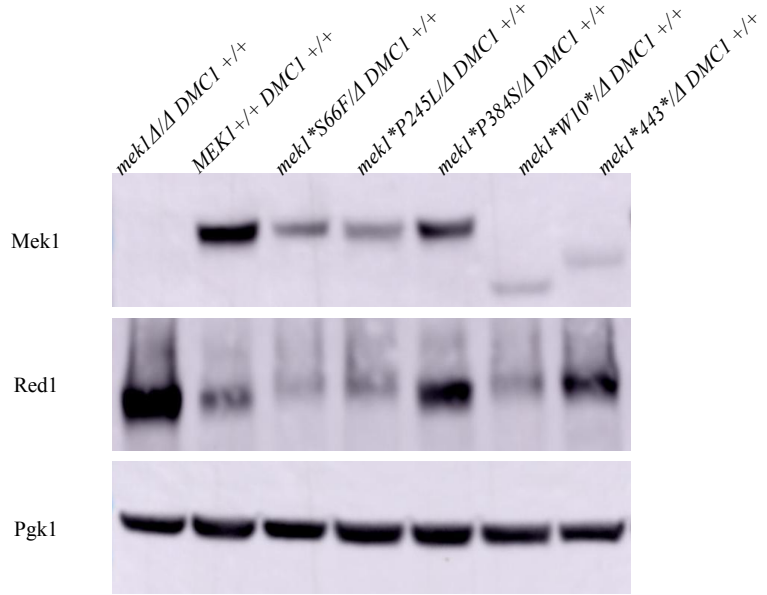

Figure 3: Mek1 protein is stably expressed in the point mutant strains.
Western blot analysis showing Mek1 protein expression for the indicated *mek1** point mutants in a *DMC1* background. Samples were taken at 4 hour time point from a synchronised meiotic cell culture. α-Red1 was used as a meiotic control and α-Pgk1 was used as a loading control.

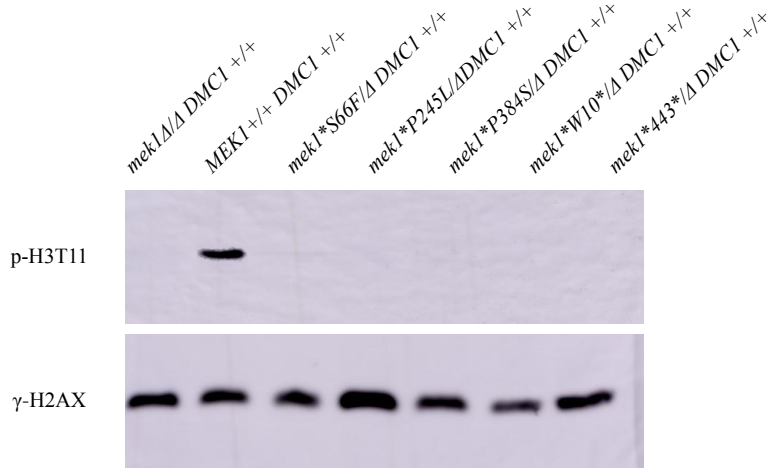

Figure 4a: Mek1 kinase activity is not observed in the point mutants

Mek1 kinase activity was monitored by the phosphorylation of Histone 3 at threonine 11. Cells harvested at 4 hour time point were resolved by SDS-PAGE and analyzed using western blot by probing with anti-phospho-H3T11 antibody for the indicated diploid strains (upper panel). Phosphorylation of γ-H2AX at Serine 129 was used as a marker for DSB formation (lower panel).

Supplementary figures

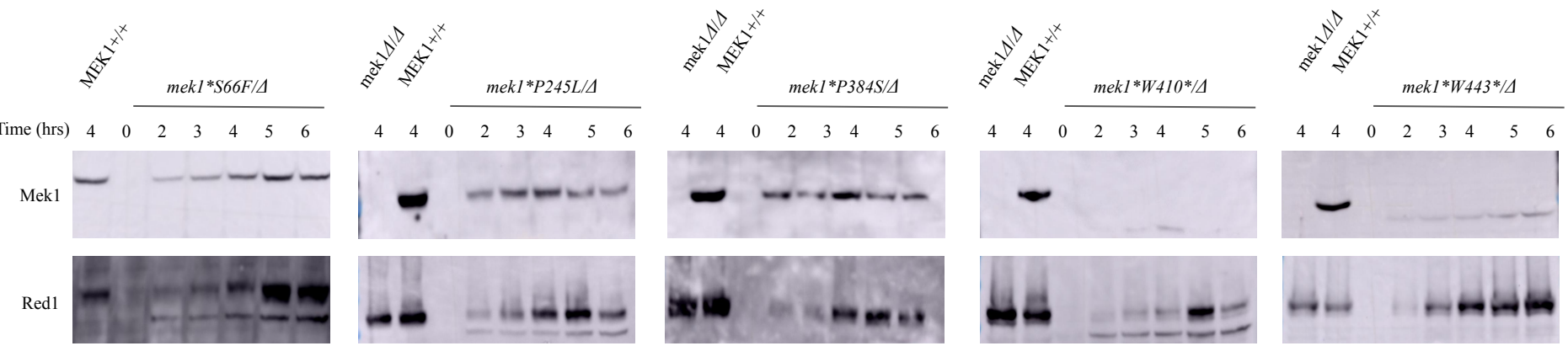

Figure S1: Mek1 expression during a time course in *mek1 point mutants**

Diploids of the indicated *mek1*/Δ* point mutants (DMC1 background) were induced to undergo meiosis in sporulation media and assayed at different time points to look at Mek1 protein expression by western blot. Red1 was used as a meiotic control. *mek1Δ/Δ* and MEK1+/+ was used as negative and positive controls respectively at 4 hour time point.

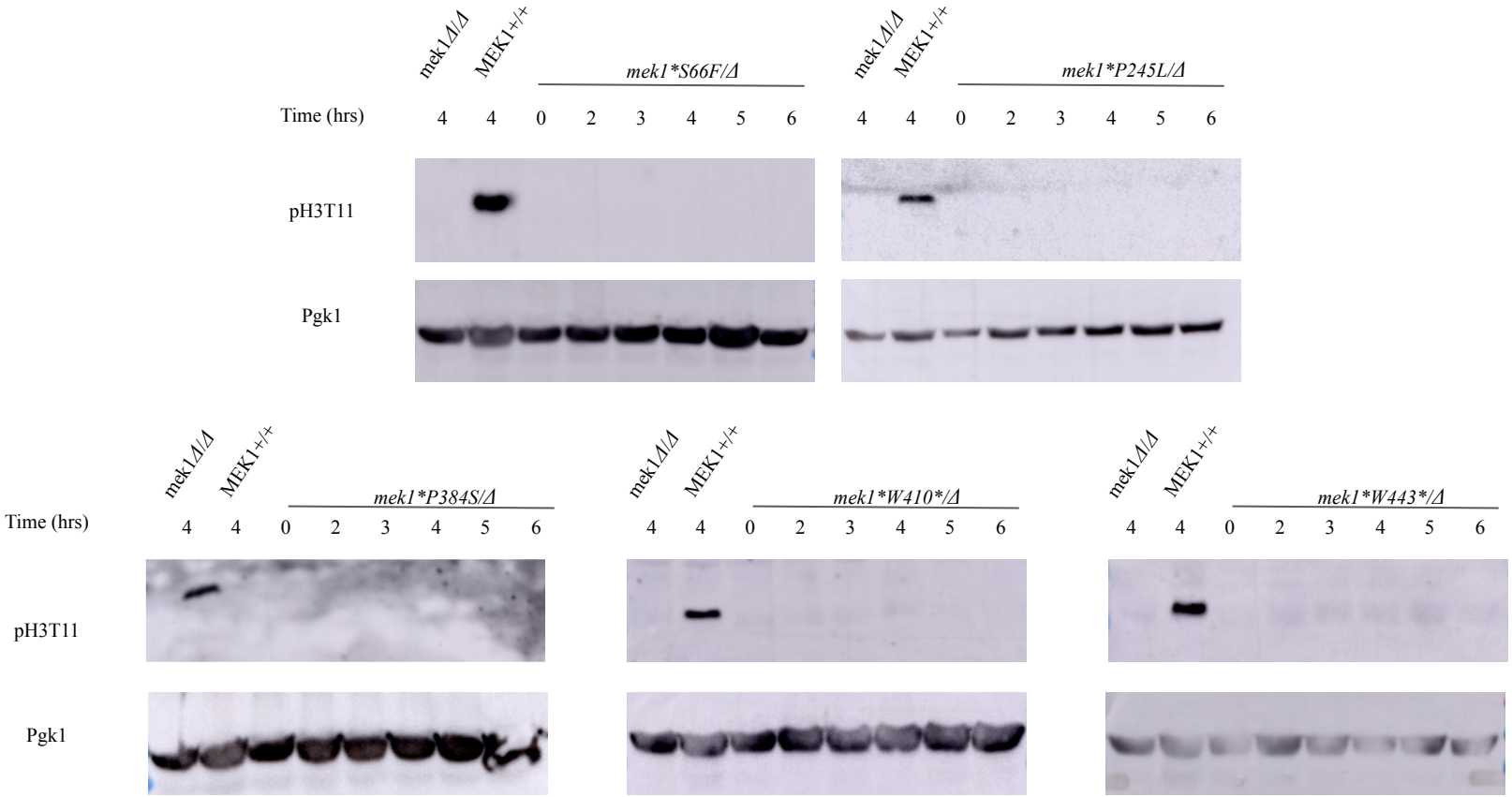

Figure S2: *mek1 point mutants are defective for H3T11 phosphorylation**

Protein extracts for the indicated diploids were assayed by western blot at different time point to look for phosphorylation of Histone3 at T11 as a readout of kinase activity of *mek1** point mutants (upper panel). Pgk1 was used as a loading control (lower panel).

Table S1: List of all *Saccharomyces cerevisiae* strains used in the study

Name	Genotype
VS8	*MATa, ho::LYS2, lys2, ura3, leu2::hisG, his3::hisG, trp1::hisG,*
VS181	*MATa, ho::LYS2, leu2::hisG, HIS4, ura3, lys2, trp1::hisG mek1Δ::kanMX*
VS298	*MATa, ho::LYS2, ura3, leu2::hisG, his3::hisG, TRP1, dmc1Δ::HIS3*
VS1690	*MATa, ho::LYS2, lys2, LEU2, his4X, ura3, TRP1 MATα, ho::LYS2, lys2, leu2::hisG, HIS3, HIS4, ura3, trp1::hisG*
VS2912	*MATα lys2, ho::LYS2, trp1::hisG, his3::hisG, leu2::hisG, ura3, dmc1Δ::HIS3, mek1Δ::HphMX4*
VS3792	*MATα lys2, ho::LYS2, trp1::hisG, his3::hisG, leu2::hisG, ura3, dmc1Δ::HIS3, mek1Δ::HphMX4 ,MATa, ,ho::LYS2, lys2, trp1::hisG,his3::hisG, leu2::hisG, ura3, dmc1::HIS3, mek1::HphMX4*
VS3793	*MATα lys2, ho::LYS2, trp1::hisG, his3::hisG, leu2::hisG, ura3, dmc1Δ::HIS3, mek1Δ::HphMX, MATa, ho::LYS2, lys2, his3::hisG, URA, LEU, TRP, ndt80Δ::TRP1, dmc1Δ::HIS3*
VS3382	*MATα lys2, ho::LYS2, trp1::hisG, his3::hisG, leu2::hisG, ura3 dmc1Δ::HIS3, mek1Δ::KanMX, ade2Δ::LEU2*
VS3383	*MATα, lys2, ho::LYS2, trp1::hisG, his3::hisG, leu2::hisG, ura3, dmc1Δ::HIS3, ade2Δ::LEU2*
VS3797	*MATa, ho::LYS2, lys2, leu2::hisG, his3::hisG, trp1::hisG dmc1Δ::HIS3, spo13::KanMX, mek1*(W410*), ura3::MATα::URA3,*
VS3798	*MATa, ho::LYS2, lys2, leu2::hisG, his3::hisG, trp1::hisG dmc1Δ::HIS3, spo13::KanMX, mek1*(P245L), ura3::MATα::URA3,*
VS3799	*MATa, ho::LYS2, lys2, leu2::hisG, his3::hisG, trp1::hisG dmc1Δ::HIS3, spo13::KanMX, mek1*(P384S), ura3::MATα::URA3,*
VS3803	*MATa, ho::LYS2, lys2, leu2::hisG, his3::hisG, trp1::hisG dmc1Δ::HIS3, spo13::KanMX, mek1*(W443*), ura3::MATα::URA3,*
VS3804	*MATa, ho::LYS2, lys2, leu2::hisG, his3::hisG, trp1::hisG dmc1Δ::HIS3, spo13::KanMX, mek1*(S66F), ura3::MATα::URA3,*
VS3806	*MATa, ho::LYS2, leu2::hisG, HIS4, ura3, lys2, trp1::hisG mek1*(W410*)*
VS3807	*MATα, ho::LYS2, leu2::hisG, HIS4, ura3, lys2, trp1::hisG mek1*(P245L)*

VS3808	*MATa, ho::LYS2, leu2::hisG, HIS4, ura3, lys2, trp1::hisG mek1*(P384S)*
VS3812	*MATa, ho::LYS2, leu2::hisG, HIS4, ura3, lys2, trp1::hisG mek1*(W443*)*
VS3813	*MATa, ho::LYS2, leu2::hisG, HIS4, ura3, lys2, trp1::hisG mek1*(S66F)*
VS3824	*MATa, ho::LYS2, leu2::hisG, HIS4, ura3, lys2, trp1::hisG mek1*(W410)* MATα, lys2, ho::LYS2, ura3, leu2::hisG, HIS4, arg4-Nsp, ade2-Bgl, mek1::LEU2*
VS3825	*MATa, ho::LYS2, leu2::hisG, HIS4, ura3, lys2, trp1::hisG mek1*(P245L) MATα, lys2, ho::LYS2, ura3, leu2::hisG, HIS4, arg4-Nsp, ade2-Bgl, mek1::LEU2*
VS3826	*MATa, ho::LYS2, leu2::hisG, HIS4, ura3, lys2, trp1::hisG mek1*(P384S) MATα, lys2, ho::LYS2, ura3, leu2::hisG, HIS4, arg4-Nsp, ade2-Bgl, mek1::LEU2*
VS3830	*MATa, ho::LYS2, leu2::hisG, HIS4, ura3, lys2, trp1::hisG mek1*(W443*) MATα, lys2, ho::LYS2, ura3, leu2::hisG, HIS4, arg4-Nsp, ade2-Bgl, mek1::LEU2*
VS3831	*MATa, ho::LYS2, leu2::hisG, HIS4, ura3, lys2, trp1::hisG mek1*(S66F) MATα, lys2, ho::LYS2, ura3, leu2::hisG, HIS4, arg4-Nsp, ade2-Bgl, mek1::LEU2*
VS3835	*MATα, lys2, ho::LYS2, ura3, leu2::hisG, HIS4, arg4-Nsp, ade2-Bgl, mek1::LEU2 , MATa, ho::LYS2, leu2::hisG, HIS4, ura3, lys2, trp1::hisG mek1Δ::kanMX*
VS3875	*MATa, ho::LYS2, leu2::hisG, HIS4, ura3, lys2, trp1::hisG mek1*(W410*), dmc1::kanMX6, MATα lys2, ho::LYS2, trp1::hisG, his3::hisG, leu2::hisG, ura3, dmc1Δ::HIS3, mek1Δ::HphMX4*
VS3876	*MATa, ho::LYS2, leu2::hisG, HIS4, ura3, lys2, trp1::hisG mek1*(P245L), dmc1::kanMX6 MATα lys2, ho::LYS2, trp1::hisG, his3::hisG, leu2::hisG, ura3, dmc1Δ::HIS3, mek1Δ::HphMX4*
VS3877	*MATa, ho::LYS2, leu2::hisG, HIS4, ura3, lys2, trp1::hisG mek1*(P384S), dmc1::kanMX6 MATα lys2, ho::LYS2, trp1::hisG, his3::hisG, leu2::hisG, ura3, dmc1Δ::HIS3, mek1Δ::HphMX4*
VS3881	*MATa, ho::LYS2, leu2::hisG, HIS4, ura3, lys2, trp1::hisG mek1*(W443*), dmc1::kanMX6 MATα lys2, ho::LYS2, trp1::hisG, his3::hisG, leu2::hisG, ura3, dmc1Δ::HIS3, mek1Δ::HphMX4*
VS3882	*MATa, ho::LYS2, leu2::hisG, HIS4, ura3, lys2, trp1::hisG mek1*(S66F), dmc1::kanMX6 MATα lys2, ho::LYS2, trp1::hisG, his3::hisG, leu2::hisG, ura3, dmc1Δ::HIS3,*

	mek1Δ::HphMX4
VS4060	*MATα, ho::LYS2, lys2, leu2::hisG, HIS3,HIS4, ura3, trp1::hisG, mek1*(P245L)::KanMX, dmc1Δ::HIS3, ade2Δ::LEU2*
VS4061	*MATa, ho::LYS2, lys2, leu2::hisG, HIS3,HIS4, ura3, trp1::hisG, mek1*(P245L)::KanMX, dmc1Δ::HIS3, ADE2*
VS4065	*MATa, ho::LYS2, lys2, leu2::hisG, (HIS3 or his3::hisG), HIS4, ura3, trp1::hisG, mek1*(W443Stop)::KanMX, dmc1Δ::HIS3*
VS4068	*MATα, ho::LYS2, lys2, leu2::hisG, (HIS3 or his3::hisG), HIS4, ura3, trp1::hisG, mek1*(S66F)::KanMX, dmc1Δ::HIS3, ade2Δ::LEU2*
VS4069	*MATa, ho::LYS2, lys2, leu2::hisG, (HIS3 or his3::hisG), HIS4, ura3, trp1::hisG, mek1*(S66F)::KanMX, dmc1Δ::HIS3*
VS4070	*MATα, ho::LYS2, lys2, leu2::hisG, his3::hisG, HIS4, ura3, trp1::hisG, mek1*(W410*)::KanMX, dmc1Δ::HIS3, ade2Δ::LEU2*
VS4071`	*MATa, ho::LYS2, lys2, leu2::hisG, HIS3, HIS4, ura3, trp1::hisG, mek1*(W410*)::KanMX, dmc1Δ::HIS3*
VS4077	*MATα, ho::LYS2, lys2, leu2::hisG, (HIS3 or his3::hisG), HIS4, ura3, trp1::hisG, mek1*(W443Stop)::KanMX, dmc1Δ::HIS3, ade2Δ::LEU2*
VS4086	*MATa, ho::LYS2, lys2, leu2::hisG, (HIS3 or his3::hisG), HIS4, ura3, trp1::hisG, mek1*(P384S)::KanMX, dmc1Δ::HIS3*
VS4105	*MATa, ho::LYS2, leu2::hisG, HIS4, ura3, lys2, trp1::hisG, mek1Δ::kanMX MATα, ho::LYS2, leu2::hisG, HIS3,HIS4, ura3, lys2, trp1::hisG, dmc1Δ::HIS3, ade2Δ::LEU2, MEK1*
VS4106	*MATa, ho::LYS2, leu2::hisG, HIS4, ura3, lys2, trp1::hisG, mek1Δ::kanMX MATα, ho::LYS2, lys2, leu2::hisG, his3::hisG, HIS4, ura3, trp1::hisG, mek1*(P245L)::KanMX*
VS4107	*MATa, ho::LYS2, leu2::hisG, HIS4, ura3, lys2, trp1::hisG, mek1Δ::kanMX MATα, ho::LYS2, lys2, leu2::hisG, his3::hisG, HIS4, ura3, trp1::hisG, mek1*(W443Stop)::KanMX*
VS4108	*MATa, ho::LYS2, leu2::hisG, HIS4, ura3, lys2, trp1::hisG, mek1Δ::kanMX MATα, ho::LYS2, lys2, leu2::hisG, HIS3, HIS4, ura3, lys2, trp1::hisG, mek1*(S66F)::KanMX*
VS4109	*MATa, ho::LYS2, leu2::hisG, HIS4, ura3, lys2, trp1::hisG, mek1Δ::kanMX MATα, ho::LYS2, lys2, leu2::hisG, his3::hisG, HIS4, ura3, trp1::hisG, mek1*(W410*)::KanMX*
VS4110	*MATa, ho::LYS2, leu2::hisG, HIS4, ura3, lys2, trp1::hisG, mek1Δ::kanMX MATα, ho::LYS2, lys2, leu2::hisG, HIS3, HIS4, ura3, lys2, trp1::hisG, mek1*(P384S)::KanMX, ade2Δ::LEU2*

Table S2a: Sporulation efficiency of *mek1* point mutants in *dmc1* background

Genotype	Strain (#)	Unsporulated	Monads	Dyads	Tetrads	N	Sporulation (%)
mek1Δ/Δ dmc1Δ/Δ	3792	9	4	2	185	200	95
MEK1+/Δ dmc1Δ/Δ	3793	200	0	0	0	200	0
*mek1*S66F/Δ dmc1Δ/Δ*	3882	18	1	25	156	200	91
*mek1*P245L/Δ dmc1Δ/Δ*	3876	23	1	16	160	200	88.5
*mek1*P384S/Δ dmc1Δ/Δ*	3877	17	2	13	168	200	91.5
*mek1*W410*/Δ dmc1Δ/Δ*	3875	17	1	22	160	200	91.5
*mek1*W443*/Δ dmc1Δ/Δ*	3881	4	1	32	163	200	98

Table S2b: Sporulation efficiency of *mek1* mutants in *DMC1* background (Set1)

Genotype	Strain (#)	Unsporulated	Monads	Dyads	Tetrads	N	Sporulation (%)
mek1Δ/Δ DMC1+/+	3835	18	3	6	163	200	86
MEK1+/+ DMC1+/+	1690	12	1	2	185	200	94
*mek1*S66F/Δ DMC1+/+*	3831	5	3	7	185	200	97.5
*mek1*245L/Δ DMC1+/+*	3825	10	3	16	171	200	95
*mek1*P384S/Δ DMC1+/+*	3826	36	1	27	136	200	82
*mek1*W410/Δ DMC1+/+*	3824	16	1	16	167	200	92
*mek1*W443/Δ DMC1+/+*	3830	24	3	9	164	200	88

Table S2c: Sporulation efficiency of *mek1* mutants in *DMC1* background (Set2)

Genotype	Strain (#)	No spores	Monads	Dyads	Tetrads	N	Sporulation (%)
mek1Δ/Δ DMC1+/+	3835	14	4	5	177	200	93
MEK1+/+DMC1+/+	4105	43	1	20	136	200	78.5
*mek1*S66F/Δ DMC1+/+*	4108	39	3	57	101	200	80.5
*mek1*P245L/Δ DMC1+/+*	4106	51	5	18	126	200	74.5
*mek1*P384S/Δ DMC1+/+*	4110	69	1	29	101	200	65.5
*mek1*W410/Δ DMC1+/+*	4109	121	0	8	71	200	39.5
*mek1*W443/Δ DMC1+/+*	4107	46	6	16	132	200	77

Table S2d: Spore viability of *mek1* mutants in DMC1 background

Genotype	4- viable	3-viable	2-viable	1-viable	0-viable	Total viable spore	N	Viability (%)
mek1Δ/Δ DMC1+/+	0	0	0	1	39	1	40	0.625
MEK1+/Δ DMC1+/+	35	4	1	0	0	40	40	96.25
*mek1*S66F/Δ DMC1+/+*	0	0	1	2	38	3	40	2.5
*mek1*P245L/Δ DMC1+/+*	0	0	0	2	38	2	40	1.25
*mek1*P384S/Δ DMC1+/+*	0	0	0	0	0	0	40	0
*mek1*W410/Δ DMC1+/+*	0	0	4	3	35	7	40	6.875
*mek1*W443/Δ DMC1+/+*	0	0	0	0	40	0	40	0

Table S3: Antibodies used in the study

Primary antibody	Dilution	Source	Secondary antibody	Dilution	Source
anti-Mek1	1:10,000	Pedro San-Segundo	anti-rabbit	1:5000	Abcam-Goat Anti-Rabbit IgG H&L (HRP) (ab6721)
ant-Red1	1: 5000	Nancy Hollingsworth	anti-rabbit	1:5000	Abcam-Goat Anti-Rabbit IgG H&L (HRP) (ab6721)
anti-phospho-H3T11	1:1000	Millipore (MC83)	anti-rabbit	1:5000	Abcam-Goat Anti-Rabbit IgG H&L (HRP) (ab6721)
anti-Pgk1	1:10,000	Thermofisher (2C5D8)	anti-mouse	1:5000	Abcam-Goat Anti-mouse IgG H&L (HRP) (ab97019)
Anti-Histone H2A (phospho S129)	1:1000	Abcam (ab15083)	anti-rabbit	1:5000	Abcam-Goat Anti-Rabbit IgG H&L (HRP) (ab6721)